Millimeter IMPATT Sources for the 130–170-GHz Range

KENNETH P. WELLER, MEMBER, IEEE, ROBERT S. YING, MEMBER, IEEE, AND DON H. LEE, MEMBER, IEEE

Abstract—**Device and circuit design of silicon IMPATT sources in the 130–170-GHz range is discussed. A 170-GHz source has been developed with 16 mW at the isolator output having an AM double-sideband noise-to-signal ratio of −115 dB per 1 kHz beyond 70 kHz from carrier.**

I. Introduction

THE potential for very-high-frequency operation using silicon IMPATT devices has been recognized since the early development period. Not long after the first demonstration of IMPATT operation, pioneering work by Bowman and Burrus led to achievement of operation up to 300 GHz in the fundamental IMPATT mode, albeit in pulsed operation [1]. With improved device fabrication technology, CW operation using diffused p^+-n IMPATT's was observed up to 151 GHz with 3.5-mW output power [2]. Recently, advancement in device technology, including the advent of the ion-implanted double-drift region IMPATT structure [3], and increased interest in millimeter systems applications have given impetus for further work to advance the power and frequency capabilities of these solid-state sources. Recently reported achievements include the generation of 85 mW with 2.8-percent efficiency at 161 GHz using diffused junction single-drift n-type diodes [4].

The present paper describes the development of IMPATT sources for operation up to 170 GHz, primarily for use as parametric amplifier pump sources. This activity has concentrated on the development of techniques for fabricating the DDR structure with good doping profile resolution. The circuit development has concentrated on performance optimization using these devices in a single-quartz-stand-off package. This work has led to the achievement of 28-mW CW output at 170 GHz.

II. Device Design and Fabrication

The DDR IMPATT profile for the devices used in this work were formed in thin n on n^+ silicon epitaxial material grown on arsenic doped ⟨111⟩ substrate wafers. The lightly doped p region is fabricated by overcompensating with implanted boron ions. Further detail on the implantation technology is published elsewhere [5]. The p^+ contact layer is formed by a shallow low-temperature diffusion. After profile formation, an array of inverted mesa diodes is fabricated from the wafer on a large-area bonded copper heat-sinking disk. The diodes are separated by a gang punch operation on the copper disk which provides each diode with a copper heat-sinking pedestal.

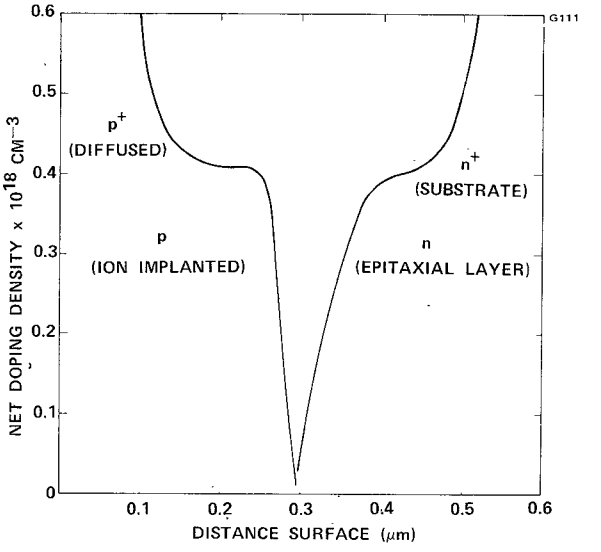

Fig. 1. IMPATT doping profile designed for 150–170-GHz range as determined from C–V measurements.

The profile design for the devices was initially based on standard transit-time consideration and was optimized empirically. The estimated profile for one of the better device lots is shown in Fig. 1. This profile was derived from capacitance–voltage (C–V) measurements on the epitaxial material before and after implantation. The profile approximates a symmetrical p^+-p-n-n^+ structure with slightly over 4×10^{17} cm^{-3} net doping density in the lightly doped regions away from the graded p-n junction region. The calculated small-signal characteristics of the active region associated with this profile are shown in Fig. 2 for both room temperature and an operating temperature of 250°C at a current density of 60 kA/cm^2. A current density near this value was required to achieve operation near 170 GHz. The avalanche coefficients reported by Grant were used to calculate these characteristics [6]. The results of Fig. 2 suggest that the optimum frequency range of operation under the indicated operating conditions is 130–170 GHz. Based on the curve for 250°C junction temperature, the small-signal device impedance for a diode of the size required for 170-GHz operation is approximately $(-2-j11)$ Ω. This estimate is for a device diameter of 20 μm. This estimate does not include the parasitic series resistance due to the contacts or the undepleted current path through the

Manuscript received February 3, 1976; revised May 6, 1976. This work was supported by the Air Force Avionics Laboratory under Contract F33615-74-C-1025.

The authors are with the Torrance Research Center, Hughes Aircraft Company, Torrance, CA 90509.

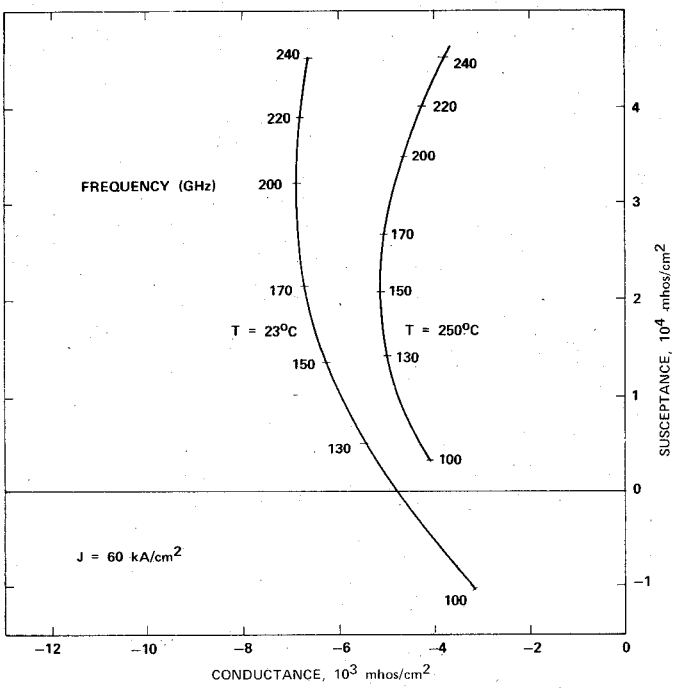

Fig. 2. Admittance characteristics for profile of Fig. 1 at 60 kA/cm² at junction temperatures of 23 and 250°C based on Grant's rates.

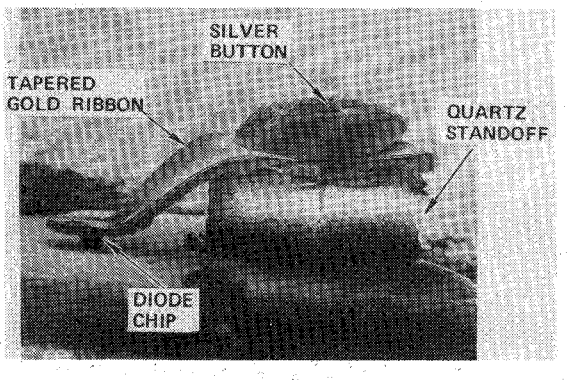

Fig. 3. Scanning electron micrograph of the quartz-standoff packaged 170-GHz IMPATT.

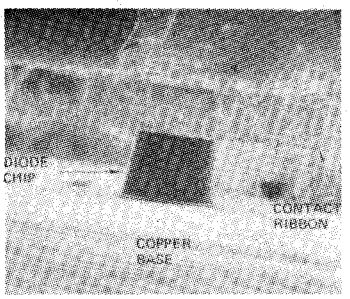

Fig. 4. Scanning electron micrograph showing a close-up of the silicon double-drift IMPATT trim etched to the size required for 170-GHz operation (~ 20-μm diameter).

silicon to the active junction region which reduces the real part of the device impedance to an even smaller value.

To achieve the desired device/circuit match, the package and circuit configuration in the proximity of the silicon chip must transform the impedance to a higher level more compatible with the characteristic impedance of the guiding structure; in this case, reduced-height rectangular waveguide. In lower millimeter bands this can be accomplished by properly designing the package dimensions to allow the quasi-lumped package network to act as an impedance inverter in the frequency range of interest. Above a certain frequency, the effective lead inductance required to do this becomes too small to realize in a conventional package arrangement.

Another approach is to provide a low impedance distributed matching transformer section between the diode and the circuit element that provides the coupling to the waveguide. We have developed a package and circuit configuration which is relatively simple to construct for use in IMPATT sources above 100 GHz. The diode is packaged as follows.

1) A quartz standoff is bonded next to the diode mesa on the large-area-bonded heat sink.

2) A preformed, tapered ribbon lead is bonded between the diode back contact and the top of the standoff.

3) A silver button is bonded on top of the standoff to protect the ribbon.

A scanning electron micrograph of a device packaged in this manner is shown in Fig. 3. The ribbon is tapered to minimize the effective lead inductance. A close-up of the silicon diode chip under the ribbon, after it has been trim etched to the diameter required for 170-GHz operation, is shown in Fig. 4. The active junction region of the device, located at the base of the silicon chip, is approximately 20 μm in diameter. With our present technology, this represents an approximate lower limit on the device size that can be reliably fabricated and packaged.

III. Circuit Design and Evaluation

To obtain efficient low-noise operation as an oscillator from a solid-state active device such as an IMPATT diode, a low-loss microwave circuit must be provided that is designed to present a circuit impedance to the diode terminals at the chip level which will optimize the power generation at the desired frequency. Both the real and imaginary part of the circuit impedance must be properly designed to match the device characteristics in the frequency range of interest. The frequency of operation is determined by the imaginary part and the generation efficiency is optimized through proper choice of the real part.

At very high frequencies, the dominant element in the imaginary part of the circuit impedance presented to the silicon chip is the effective inductance of the lead ribbon in the quartz-standoff package. Although every effort has been made to minimize this inductance, the value remains too large to achieve the proper device/circuit matching to the reduced-height waveguide section. Therefore, to optimize the power performance of a source at 130–170 GHz, it is necessary to provide additional impedance matching between the package and the reduced-height waveguide load. The bias-pin resonator circuit was conceived to

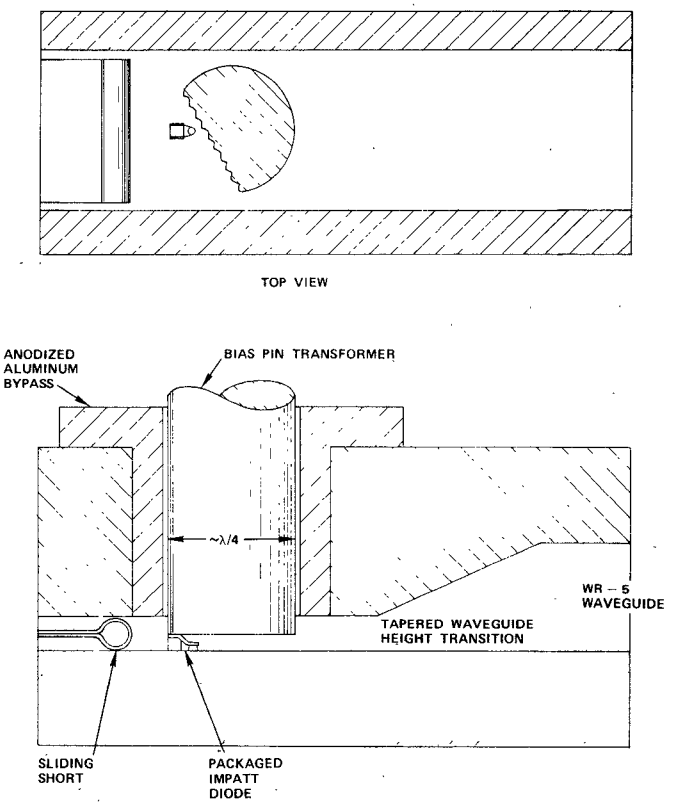

Fig. 5. Bias-pin resonator waveguide circuit configuration.

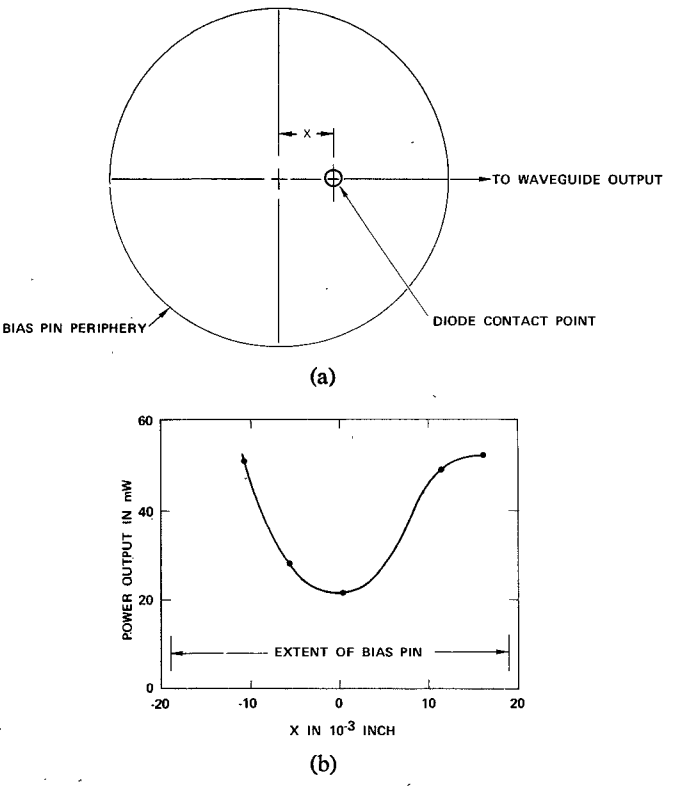

Fig. 6. IMPATT performance as a function of diode contact point on bias pin of circuit shown in Fig. 5. (a) Diagram defining diode contact point X. (b) Power output versus diode contact point X.

provide the required impedance transformation. A schematic cross section of the bias-pin arrangement is given in Fig. 5. The key element in this circuit that differentiates it from conventional circuits of this type is the relatively large bias-pin diameter. The IMPATT diode is contacted near the rear edge of the pin. In this configuration the lower face of the bias pin forms an open cavity with the lower broad wall of the waveguide which, at the cavity resonance, provides a matching function between the IMPATT diode and the waveguide load. The use of this bias-pin resonator also minimizes the effective lead inductance of the tapered ribbon connecting the diode to the standoff by placing the ribbon between two conducting planes. The distributed capacitance between the ribbon and the bias pin on one side, and the ground plane on the other, minimizes the effective inductance. An additional benefit of the bias-pin resonator configuration is the ease of circuit fabrication.

A. Circuit Optimization

Choice of the design parameters has been accomplished through an intuitive understanding of the circuit behavior and use of empirical design information gained by testing a diode in several circuits for which a parameter is systematically varied. The primary circuit design parameters are waveguide height and width, bias-pin diameter, and diode contact position. A series of experiments were conducted to observe the effects on oscillator operation of varying each of these parameters.

A study of the performance of one diode as a function of position under the bias pin was conducted using a special diode heat sink constructed for this purpose. The results are summarized in Fig. 6. The power output and frequency of a diode under fixed bias conditions was measured as a function of the distance X between the center line of the bias pin and the diode-standoff contact point. As indicated in Fig. 6(a), the position was varied from near the rear edge of the pin closest to the sliding short (negative X) to near the front edge. As can be seen from Fig. 6(b), the position of contact is an important factor in the operation of this circuit. Best performance is generally obtained with contact near the rear edge of the pin, although contacting near the front edge can also produce clean efficient operation. Contacting near the center of the pin generally results in noisy output at a relatively low power. The frequency of operation was found to be insensitive to the position of contact. The frequency for the data of Fig. 6(b) is between 136 and 137 GHz for all points. Based on these results, experimental circuits were designed with the diode contact at the rear edge of the bias pin, as shown in Fig. 5, regardless of the pin diameter. Three parameters were varied in this basic configuration in order to increase the oscillation frequency. These are as follows.

1) *Bias-Pin Diameter:* The bottom face of the bias pin serves as a resonant element for impedance transformation for a pin diameter on the order of a quarter-wavelength at resonance. By decreasing pin diameter, the resonant frequency increases. Of course, this is an oversimplified view of the situation in the case of a packaged device since the package parasitics dominate the oscillator behavior.

2) *Waveguide Width:* One way to decrease the inductance of the lead ribbon connecting the diode's back contact to the standoff is to reduce the waveguide width while holding

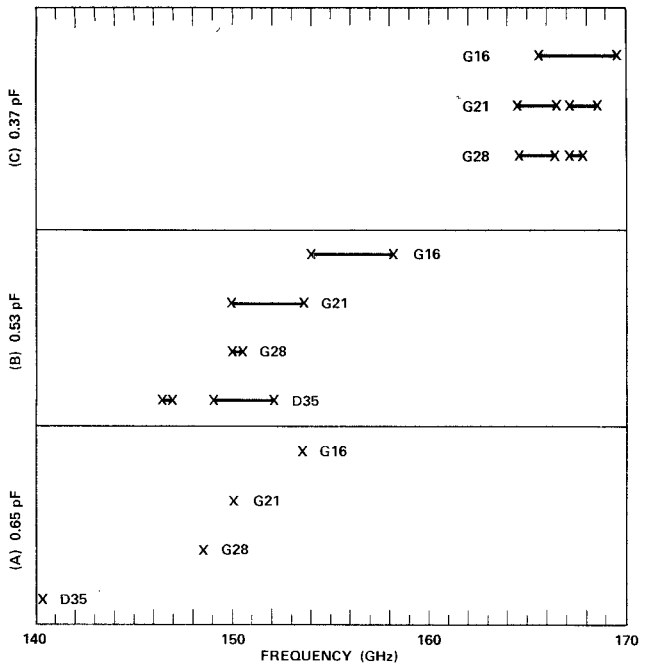

Fig. 7. Tuning range as a function of bias-pin diameter for three diodes from the same lot having different zero-bias capacitance and bias conditions as follows. (A) 0.65 pF, $I = 300$ mA. (B) 0.53 pF, $I = 275$ mA. (C) 0.37 pF, $I = 220$ mA.

the lead length constant. This can be understood qualitatively from the formula for a centered inductive post of diameter d and length l in waveguide of width W given by

$$L = 2l \ln\left(\frac{4W}{\pi d}\right) \text{ nH/cm.} \quad (1)$$

From this it is apparent that the inductance is reduced as waveguide width is reduced for fixed post dimensions. This formula is derived for a centered post extending completely across a waveguide, but qualitatively the same behavior is observed in the 50–100-GHz range for packaged IMPATT diodes in the conventional small-diameter-bias-pin circuit. The relatively large diameter of the bias pin in the bias-pin resonator circuit tends to shield the effect of the waveguide sidewalls on the package inductance, but some frequency tuning is still observed.

3) Diode Area: Reducing the diode area is the most obvious way to increase oscillation frequency. The device capacitance is decreased in this manner, thereby increasing the frequency at which device and circuit reactance cancel one another. Of course, decreasing the diode area also limits the power handling capability of the device, which is undesirable.

Three diodes from the same processed wafer were tested in several circuits to clearly illustrate the aforementioned behavior. In Fig. 7 the test results are summarized in terms of operating frequency range for a given zero-bias diode capacitance and circuit. A mechanical tuning range is indicated by a line with X's marking the end points. The diodes were chosen to have significantly different capacitances to illustrate the effect of diode capacitance on operating frequency. Four circuits were used to test the diodes, all of which have a reduced-height section of 0.010 in that contains the diode and bias assembly. A linear taper to full height is used for matching to the waveguide load. A movable short is placed behind the diode in the reduced-height section. The mechanical frequency tuning is accomplished by moving this short. Three of the circuits were built for *G* band (WR5 waveguide of dimensions 0.051 × 0.0255 in) and one for *D* band (WR-7 waveguide of dimensions 0.065 × 0.0325 in). The bias-pin diameter for each circuit is given beside each point or curve in Fig. 7 in thousandths of an inch, i.e., G 28 is the *G*-band circuit with a 0.028-in-diam bias pin.

For each diode and circuit the oscillator performance was tested over the full range of tuning provided by the movable short, while the diode bias conditions were fixed. No fine tuning was provided in front of the diode. In some cases the frequency of oscillation could be continuously tuned over one or more range of frequency; in other cases the frequency was essentially fixed. The latter situation is indicated in Fig. 7 by a single X marking the single oscillation frequency. Generally, diodes with a smaller junction area were more mechanically tunable, as is apparent from Fig. 7. The 0.65-pF diode tested could not be mechanically tuned in any of the circuits by moving the short, but the frequency could be varied over a large range by changing the dimension of the bias-pin resonator and waveguide width. The bias-pin dimension is less dominant in determining frequency for the smaller diodes because the frequency can be tuned mechanically over a significant range. The trend still exists, though, for the tuning range to shift up in frequency for decreasing pin diameter. The power variation within the tuning ranges indicated in Fig. 7 is 3 dB or less with the maximum power point generally falling near the middle of the tuning range. To optimize power for a given frequency requires proper choice of the pin diameter as well as the device area. The amount of tuning we have been able to achieve by varying the circuit parameters is significant, but it is much smaller than can be achieved if the package parasitics can be reduced.

B. Power Measurements

Because of the limited amount of activity in the frequencies much above 100 GHz, accurate measurement of a basic quantity such as power becomes difficult. It is therefore worthwhile to discuss to some extent the techniques we have used to make these measurements in the 130–170-GHz range. Power measurements would normally be made using a thermistor mount which can be calibrated against a more accurate standard such as a calorimeter. Because a thermistor responds to changes in power relatively fast, it is more suitable than a slow-responding calorimeter for continuous power monitoring of a source during tuning. A Schottky barrier or point contact detector responds rapidly also, but the sensitivity of the detector is usually a stronger function of frequency, making calibration difficult.

Initially, we used a Hitachi T1511 thermistor mount constructed in WR-7 (*D*-band) waveguide and calibrated from 134–145 GHz at the factory. The assumption was made that the thermistor correction factor would increase monotonically for frequencies above 145 GHz. Later we

calibrated the thermistor at several points in the range 145–165 GHz against a Hitachi Model E3904 dry calorimeter constructed in WR12 waveguide. A transition was used from WR12 to WR7 for the purpose of injecting the high-frequency power. The return loss looking into the transition was over 25 dB. The calorimeter had been calibrated against other standards at 60 and 90 GHz. The sensitivity at both frequencies was measured to be 40.75 μV/mW. It was assumed that the same sensitivity exists at frequencies up to 170 GHz. In fact, the sensitivity may decrease for higher frequencies due to increased losses. Our assumption of constant sensitivity therefore yields a conservative power calibration factor using the calorimeter. The transition loss from WR12 to WR7 was measured using two back-to-back transitions. The correction for this loss lies between 0.2 and 0.3 dB over the entire frequency range of interest (130–170 GHz). We found that the correction factor for the Hitachi thermistor mount increases abruptly above 146 GHz. In the range above 160 GHz the correction varies by as much as 2 dB for relatively small changes in frequency. Because this behavior made the thermistor of little value in making power determinations above 145 GHz, the calorimeter was used directly to measure power. The loss in the measurement line between the IMPATT source and the calorimeter was measured at each frequency by direct substitution. The IMPATT oscillator itself was used as a source by heavily padding it to insure that the IMPATT was not detuned during the process of substitution. An attenuation of over 17 dB was placed between the IMPATT and the power reference plane. A relative measurement of power at the reference plane, and with the line inserted between the reference and the power detector, was then made to determine the line loss. Performing this measurement at each frequency insured that an error in calculated power due to line-loss variation with frequency was not made.

Extensive performance data have been taken in the frequency range 130–170 GHz using the calibrated thermistor or calorimeter directly where appropriate for power determination. The best data are summarized in Fig. 8 where the best power achieved is plotted as a function of frequency. In terms of power X (frequency)^2 product the best point is 80 mW at 139 GHz. As the frequency increases, the power output falls more rapidly than predicted by the Pf^2 law; the dependence approximates a $Pf^{4.3}$ behavior. The rapid drop in power and efficiency with increasing frequency is believed to result primarily from the difficulty in properly matching the device impedance with the present standoff package. Because of the large lead inductance, the device area must be reduced more than is assumed in the Pf^2 derivation to increase the frequency much beyond 140 GHz.

C. AM Noise Detection

For some applications, such as parametric amplifier pumps and local oscillators, the AM noise performance of the source is of utmost importance. We have employed the direct detection method to measure the AM noise performance of sources constructed for operation up to 170 GHz [7], [8]. The key element in the measurement system is a low-noise high-sensitivity Schottky-barrier detector. Details on the device fabrication and basic circuit configuration utilized in the construction of this detector have been reported previously [9]. The design was scaled in size to construct a detector in WR5 waveguide. At 170 GHz the detector constructed has a sensitivity, unloaded, of 400 mV/mW at a 0.25-mW drive level, which is comparable in performance to millimeter detectors constructed for the 50–100-GHz range. In the AM noise measurement, the detector is used to mix the AM noise sidebands on the incoming carrier with the carrier frequency to generate an IF noise voltage which is amplified and measured. The detector has been characterized as a mixer in the 140-GHz range. For a local-oscillator drive level of 3 mW, a single-sideband conversion loss of 9 dB was measured for an intermediate frequency of 1.35 GHz. The performance of this detector was more than adequate to measure the noise levels present in the IMPATT source.

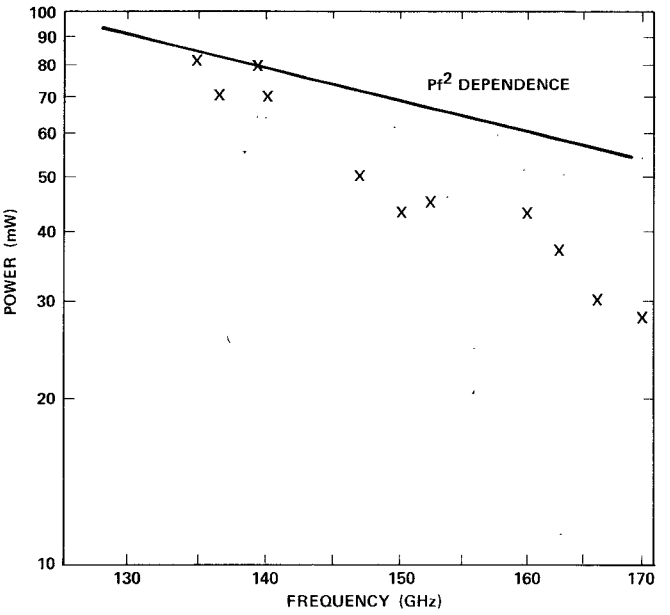

Fig. 8. Logarithmic plot of power versus frequency for double-drift IMPATT's operated in the 130–170-GHz range in the bias-pin resonator circuit.

D. 170-GHz Source Construction

To demonstrate the feasibility of constructing practical hardware in the 170-GHz range, an experimental pump source was constructed for 170-GHz operation, which was provided with an isolator at the output. This source delivers 16 mW at the isolator output and is insensitive to load conditions. The close-to-carrier AM noise spectrum of the source has been characterized from 1 kHz to 1 MHz from carrier, and is plotted in Fig. 9. Beyond 70 kHz from the carrier, the double-sideband signal-to-noise ratio referenced to a 1-kHz window is better than 115 dB. Below 70 kHz from carrier the noise increases with an approximate $1/f$ dependence. The noise behavior is comparable with lower frequency millimeter IMPATT sources.

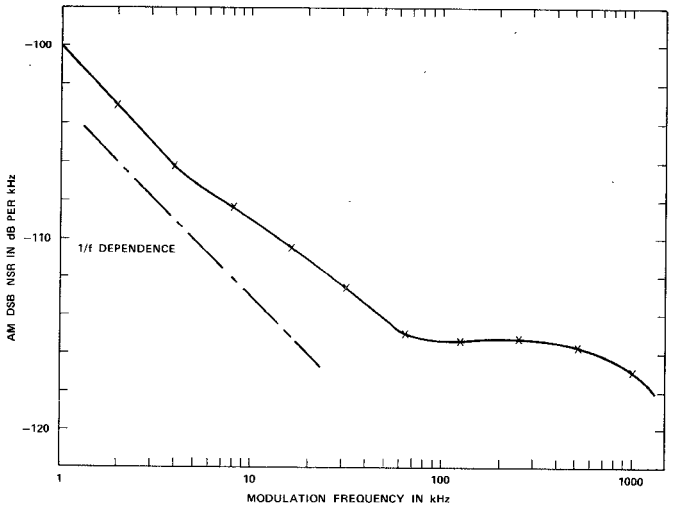

Fig. 9. AM noise spectrum of the experimental 170-GHz source presented in terms of double-sideband noise-to-signal ratio for a 1-kHz noise bandwidth as a function of distance from carrier.

An estimation of the mean-time-to-failure for the 170-GHz IMPATT source can be made based on the extensive reliability studies conducted on silicon IMPATT's [10]. The rise in junction temperature above ambient for the 170-GHz IMPATT biased to 185 mA is estimated to be 240°C. This is the bias level required to generate 16 mW at the isolator output. For an ambient of 25°C the MTFB predicted at this bias is 1.8×10^4 h.

IV. Conclusion

Utilizing highly refined, but essentially conventional, device fabrication techniques, practical CW operation of IMPATT sources has been extended to 170 GHz. A simple bias-pin resonator circuit has been developed to compensate as much as possible for the undesired package parasitics of the quartz-standoff diode package. In this configuration, the best power attained drops sharply with frequency beyond 140 GHz. We believe that significant further improvement in power in this frequency range or extension in operation beyond 170 GHz will require the development of much improved device fabrication and packaging technology to reduce the parasitics. In particular, the development of a "direct contact" configuration which eliminates the need for a quartz standoff and lead ribbon is desired. However, the construction of such a "packageless" configuration must be consistent with typical mechanical ruggedness and reliability requirements for it to be of any practical importance.

Acknowledgment

The authors wish to thank R. L. Bernick and H. C. Bowers for assistance in the small-signal device computer modeling. They also wish to thank E. M. Nakaji, A. E. Martin, and M. G. Padilla for their technical assistance in device fabrication, and H. H. Luckey and G. C. Oransky for assistance in microwave testing.

References

[1] L. S. Bowman and C. A. Burrus, "Pulsed-driven silicon p-n junction avalanche oscillators for the 0.9 to 20 mm band," *IEEE Trans. Electron Devices*, pp. 411–418, August 1967.
[2] T. Misawa and L. P. Marinaccio, "100 GHz Si IMPATT diodes for CW operation," *Proc. Symposium on Submillimeter Waves*, pp. 53–67, 1970.
[3] T. E. Seidel and D. L. Scharfetter, "High power millimeter-wave IMPATT oscillators with both hole and electron drift spaces made by ion implantation," *Proc. IEEE*, pp. 1135–1136, July 1970.
[4] M. Ohmori, M. Hirayama, and T. Ishibashi, "150 GHz band IMPATT oscillators, frequency converters, and doublers," *Proceedings of 1975 International Microwave Symposium*, pp. 219–221, May 1975.
[5] D. H. Lee *et al.*, "Ion-implanted profiles for high-frequency (> 100 GHz) IMPATT diodes," *4th International Conf. Ion Implantation in Semiconductors and Other Materials*, pp. 167–168, Osaka, Japan.
[6] W. N. Grant, "Electron and hole ionization rates in epitaxial silicon at high electric fields," *S.S. Electronics*, pp. 1189–1203, 1973.
[7] J. G. Ondria, "A microwave system for measurement of AM and FM noise spectra," *IEEE Trans. Microwave Theory Tech.*, vol. MTT-16, pp. 767–781, Sept. 1968.
[8] K. P. Weller, "A study of millimeter-wave GaAs IMPATT oscillator and amplifier noise," *IEEE Trans. Electron Devices*, vol. ED-20, pp. 517–521, June 1973.
[9] H. M. Leedy *et al.*, "Advanced millimeter-wave mixer diodes, GaAs and silicon, and a broadband low-noise mixer," *Proceedings Third Cornell Conf. on High Frequency Generation and Amplification*, pp. 451–462, August 1971.
[10] R. L. Bernick, private communication.